# Phosphoproteomic profiling highlights CDC42 and CDK2 as key players in the regulation of the TGF-β pathway in *ALMS1* and *BBS1* knockout models

Brais Bea-Mascato[1,2], Girolamo Giudice[3], Iguaracy Pinheiro-de-Sousa[3], Carlos Solarat [1,2], Evangelia Petsalaki[3], Diana Valverde[1,2]

[1] CINBIO, Universidad de Vigo, 36310, Spain.

[2] Grupo de Investigación en Enfermedades Raras y Medicina Pediátrica, Instituto de Investigación Sanitaria Galicia Sur (IIS Galicia Sur), SERGAS-UVIGO, Vigo, Spain

[3] European Molecular Biology Laboratory-European Bioinformatics Institute, Wellcome Genome Campus, Hinxton CB10 1SD, UK

Correspondence: Diana Valverde

CINBIO Facultad de Biología, Universidad de Vigo, Campus As Lagoas-Marcosende s/n, 36310 Vigo, Spain

Tel +34 986 811 953

Email: dianaval@uvigo.es

# ABSTRACT:

**BACKGROUND:**

The primary cilium is a sensory organelle that extends from the plasma membrane. It plays a vital role in physiological and developmental processes by controlling different signalling pathways such as WNT, Sonic hedgehog (SHh), and transforming growth factor β (TGF-β). Ciliary dysfunction has been related to different pathologies such as Alström (ALMS) or Bardet-Biedl (BBS) syndrome. The leading cause of death in adults with these syndromes is chronic kidney disease (CKD), which is characterised by fibrotic and inflammatory processes often involving the TGF-β pathway.

**METHODS:**

Using genomic editing with CRISPR-CAS9 and phosphoproteomics we have studied the TGF-β signalling pathway in knockout (KO) models for *ALMS1* and *BBS1* genes. We have developed a network diffusion-based analysis pipeline to expand the data initially obtained and to be able to determinate which processes were deregulated in TGF-β pathway. Finally, we have analysed protein-protein interactions to prioritise candidate genes in the regulation of the TGF-β pathway in Alström and Bardet-Biedl syndrome.

**RESULTS:**

Analysis of differentially phosphorylated proteins identified 10 candidate proteins in the *ALMS1* KO model and 41 in the *BBS1* KO model. After network expansion using a random walk with a restart model, we were able to obtain processes related to TGF-β signalling such as endocytosis in the case of *ALMS1* or extracellular matrix regulation in *BBS1*. Protein interaction analyses demonstrated the involvement of CDC42 as a central protein in the interactome in *ALMS1* and CDK2 in the case of *BBS1*.

**CONCLUSION:**

In conclusion, the depletion of *ALMS1* and *BBS1* affects the TGF- β signalling pathway, conditioning the phosphorylation and activation of several proteins, including CDC42 in the case of *ALMS1* and CDK2 in the case of *BBS1*.


**KEYWORDS:** ALMS1, BBS1, ciliopathies, TGF-β, phosphoproteomics, Alström syndrome, Bardet-Biedl syndrome.

# INTRODUCTION:

The primary cilium is a microtubule-based sensory organelle that extends from the plasma membrane. It is present in all cell types and plays a vital role in physiological and developmental processes by controlling different signalling pathways such as WNT, Sonic hedgehog (SHh), and transforming growth factor β (TGF-β) (Berbari et al., 2009; Ishikawa and Marshall, 2011; Christensen et al., 2012; May-Simera et al., 2018; Anvarian et al., 2019). Ciliary dysfunction generates different phenotypes, the most common of which are obesity, type 2 diabetes mellitus, retinopathies or the appearance of multi-organ fibrosis leading to liver, kidney, or lung dysfunction (Gerdes et al., 2009; Waters and Beales, 2011; Reiter and Leroux, 2017; May-Simera et al., 2018).

The group of diseases characterised by ciliary dysfunction, mutations in primary cilium or basal body genes, are commonly known as ciliopathies. Alström syndrome (ALMS) and Bardet-Biedl syndrome (BBS) are two model ciliopathies where, despite the progress made in recent years, a clear pathological mechanism has not yet been established. (Forsythe and Beales, 2012; Forsythe et al., 2018; Hearn, 2018). ALMS is a monogenic recessive disease with an incidence of 1 in 1,000,000 individuals in the general population. To date, the only known causative gene is the *ALMS1* gene, which codes for a centrosome-associated protein, responsible for maintaining cohesion between the mother centriole and the daughter centriole (Collin et al., 2002; Hearn et al., 2005; Marshall et al., 2011). On the other hand, BBS is also an autosomal recessive disorder, with 23 causative genes described to date, named from *BBS1* to *BBS23*, being BBS1 the most prevalent gene with mutations in 23% of described cases (Forsythe and Beales, 2012; Forsythe et al., 2018). The main proteins of BBS, BBS1, BBS2, BBS4, BBS5, BBS7, BBS8, BBS9 and BBS18/BBSIP1, encode for an octameric protein complex called the BBSome involved in primary cilia transport (IFT), retrograde and anterograde (Klink et al., 2020; Singh et al., 2020). The clinical phenotypes of these two ciliopathies are overlapping, making their differentiation difficult and complicating the correct diagnosis (Aliferis et al., 2012). One of the main causes of death in adult patients with these syndromes is chronic kidney disease (CDK) (Li et al., 2007; Marshall et al., 2011; Putoux et al., 2012; Jaykumar et al., 2018; Waldman et al., 2018; Baig et al., 2020; Meyer et al., 2022). This disease is usually accompanied by inflammatory and fibrotic processes that

78 progressively degrade normal kidney function until eventually renal failure and death
79 occur (Meng et al., 2014).

80 The TGF-β pathway is one of the main pathways involved in fibrotic and inflammatory
81 processes at the cellular level (Lan, 2011; Finnson et al., 2020). It is related to the control
82 of several processes such as mitosis, apoptosis, cell migration or autophagy through
83 cross-signalling with other pathways such as MAPK, PI3K/AKT or SMADs (Massagué,
84 2012; Hamidi et al., 2017; Luo, 2017; Zhang et al., 2017; Gasior et al., 2019). In previous
85 studies in our laboratory, we have determined that *ALMS1* depletion leads to altered
86 signal transduction of the TGF-β pathway and other related pathways such as AKT or
87 p53 (Álvarez-Satta et al., 2021; Bea-Mascato et al., 2022b, 2022a), altering processes
88 such as cell migration or EMT. In this study, we apply an original approach based on
89 phospho-proteomics to delve into the regulation of the TGF-β pathway in ALMS and to
90 determine for the first time whether there are alterations in this pathway in BBS.

# MATERIALS AND METHODS:

## Cell culture and CRISPR knockouts:

The hTERT-BJ-5ta cell line, provided by the American Type Culture Collection (ATCC), was maintained in a medium composed of 4:1 of Dulbecco's minimal essential medium (DMEM, Gibco, Invitrogen, NY, USA) and Medium 199, Earle's Salts (Gibco, Invitrogen, NY, USA), supplemented with 10% fetal bovine serum (FBS) (Gibco, Invitrogen, NY, USA) and 2% penicillin/streptomycin (P/S) (Gibco, Invitrogen, NY, USA). In this study, a knockout model for the *BBS1* gene was generated **(Figure S1 A, B)** using 4 different sgRNAs **(Supplementary Table S1-2)** and a knockout (KO) model for the *ALMS1* gene previously generated in Bea-Mascato et al (Bea-Mascato et al., 2022b) was used. The methodology used in the generation of the *BBS1* model was the same as described in Bea-Mascato et al (Bea-Mascato et al., 2022b).

## TGF-β stimulation and protein extraction:

Cell lines were cultured in 150 mm dishes (Corning, NY, USA) until 90% confluence was reached and then serum starved for 24 hours. The following day, rhTGF-β1 ligand (R&D Systems; 240-B) was added to the plates at a final well concentration of 2ng/mL for 0 and 30 min. The plates were then washed 3 times with PBS and the cells were harvested in a volume of 1.5mL of PBS. They were then pelleted at 10000 rpm for 5 minutes in a Sigma® 1-14 K at 4°C. The PBS volume was removed from the tubes and the pellets were frozen at -80C until the experiment was continued.

Protein extraction was performed by adding 500µL of TEAB 100mM lysis buffer with 1% SDS (Thermo Fisher, Waltham, USA) to each sample. Samples were sonicated by giving five 5-second pulse intervals with a wave amplitude of 20% on a Branson ultra sonicator model 102C (Branson Ultrasonic, Connecticut, USA). They were then left to stand on ice for 10 minutes with moderate agitation. Finally, the cell debris was removed by centrifuging the samples for 30 minutes at 12000rpms in a Sigma® 1-14 K at 4°C. The supernatant from the tubes was transferred to low-binding tubes (Thermo Fisher, Waltham, USA) and stored at -80 degrees until the next step of the analysis.

119 Quantification of protein lysates was performed using the Pierce™ BCA Protein Assay Kit
120 (Thermo Fisher, Waltham, USA).

# 121 Reduction, alkylation and precipitation:

122 Initially, samples were centrifugated at 16,000 rpm for 10 min at 4°C. Then, 600µg per
123 sample was transferred into a new 1.5 mL tube and adjusted to a final volume of 600µL
124 with 100mM TEAB buffer. Samples were divided into several tubes (200µL/tube). 10µL
125 of 200mM TCEP was added to each tube and incubated at 55°C for 1 hour. Then, 10µL
126 of 375mM iodoacetamide (IAA) was also added to the sample and incubated for 30
127 minutes protected from light at room temperature (RT). Finally, 6 volumes (1200µL) of
128 acetone pre-cooled to -20 degrees were added and left to precipitate overnight. The
129 next day the samples were centrifuged at 8000rpms for 12 min at 4°C, the acetone was
130 decanted off and the pellet was left to dry for 2-3 min.

# 131 Protein digestion and cleaning, $TiO_2$ enrichment, 132 TMT labelling and LC-MS/MS analysis:

133 Approximately 200µg of protein pellets precipitated in acetone were resuspended with
134 200 µL of 100mM TEAB buffer. Then 5µL (5µg) of trypsin was added per tube and
135 digested at 37°C overnight. The next day, 10 µL of 5% trifluoroacetic acid (TFA) was
136 added to reduce the pH of the solution. Finally, peptide samples were cleaned up using
137 C18 desalting tips (Agilent OMIX 100 µL, SPE with pipette) and the pooled eluents with
138 speed-vac at 45°C. Phosphopeptide enrichment was performed using $TiO_2$ spin tips from
139 the High-SelectTM $TiO_2$ Phosphopeptide Enrichment Kit following the manufacturer's
140 protocol (Thermo Fisher, Waltham, USA). After enrichment, a further cleaning was
141 performed using C18 desalting tips.

142 Samples were resuspended in 50 µL of 100mM TEAB buffer and 20 µL of TMT label
143 reagent was added to each sample, using TMT10plex™ Isobaric Mass Tagging Kit
144 (Thermo Fisher, Waltham, USA). Samples were multiplexed and analyzed by LC-MS/MS
145 using a 90-minute gradient on Orbitrap Eclipse (Thermo Fisher, Waltham, USA) with a
146 method using CID-MSA for the identification of MS2 and a real-time search algorithm to
147 quantify reporters in MS3. As a quality control, the BSA controls were digested in parallel

148 and ran between each of their samples to avoid carryover and assess instrument
149 performance.

# 150 Protein identification and differential 151 phosphorylation analysis:

152 The identification of peptides/proteins was performed using the software Proteome
153 Discoverer software (v2.5) **(Supplementary Table S3-4)**. Samples were searched against
154 the SP_Human database (March 2021), using the search algorithm Mascot v2.6
155 (http://www.matrixscience.com/). Peptides have been filtered based on FDR and only
156 peptides showing an FDR lower than 5% have been retained. The peptides were grouped
157 into proteins with the default option of Proteome discovery (v2.5) and these were used
158 in the downstream analysis.

159 The proteins resulting from the identification were used for differential phosphorylation
160 analysis. Each multiplexed/batch (with and without stimulation of the TGF-β pathway)
161 was analysed individually with the R (v4.2.1) package DEP (Zhang et al., 2018). The data
162 was filtered to keep only the proteins that were quantified in all samples of at least one
163 condition. Subsequently, the normalization of the data by variance stabilizing
164 transformation (VSN) was performed. Finally, for data imputation, the MiniProb
165 algorithm was used with a q-value of 0.01. The log2 fold change (FC) of the differentially
166 phosphorylated proteins was calculated against the controls (WT) of the corresponding
167 batch for both knockouts (*ALMS1* and *BBS1*) **(Supplementary Table S5-6)**. For
168 downstream analyses, the differentially phosphorylated protein was that with a value
169 of $|\log2FC| > 0.5$ and an $FDR < 0.05$.

# 170 Network diffusion, enrichment analysis and protein-171 protein interaction analysis:

172 For network diffusion analysis, a graph covering the entire human interactome was
173 created with the R package, igraph (Csardi and Nepusz, 2006). The creation of the human
174 interactome was performed as follows. Initially, the human interactome was extracted
175 from the IntAct database (version: 4.2.17, last updated May 2021) (Orchard et al., 2014).

176 In addition, kinase-substrate interactions and kinase-kinase interactions contained in
177 PhosphoSitePlus (Orchard et al., 2014) (version 6.5.9.3, last update May 2021),
178 OmniPath (Türei et al., 2016) (last version May 2021) and SIGNOR 2.0 (Licata et al., 2020)
179 (last version May 2021) were integrated in this interactome. All proteins not annotated
180 in Swiss-Prot (UniProt, 2021) and those not annotated with at least one GO term (Gene
181 Ontology, 2021) were removed. The resulting protein interaction network (PIN)
182 comprised a total of 16,407 nodes and 238,035 edges. The weight of edges was defined
183 by the semantic similarity between gene pairs, modelled according to Topological
184 Clustering Semantic Similarity (TCSS) algorithm (Jain and Bader, 2010) and calculated
185 using the Semantic Measure Library (Harispe et al., 2014). The networks were
186 normalised to avoid hub bias using "correct.for.hubs" option in diffusR.

187 The differentially phosphorylated proteins detected in the previous step were used as
188 seed nodes in the interactome graph. These nodes were assigned the same weight and
189 a weight of 0 to the rest of the network. Finally, the random walk with restart (RWR)
190 algorithm (Tong et al., 2006; Köhler et al., 2008) was used through the R package diffusR
191 using a restart probability of 0.3, 10,000 iterations and a threshold of 1e-06. Nodes were
192 ordered by RWR score after diffusion, and the top 100 were used in downstream
193 analyses **(Supplementary Table S7-8)**.

194 The enrichment analysis was performed using the R package enrichR, an R interface for
195 accessing the enrichR database (Kuleshov et al., 2016). The differentially phosphorylated
196 proteins and the 100 nodes with the highest RWR scores were compared with the GO
197 Molecular Function 2021, GO Biological Process 2021, BioPlanet 2019, KEGG 2021
198 Human and MSigDB Hallmark 2020 datasets. Only the 20 processes with the lowest FDR
199 were considered using an FDR < 0.05 as a threshold.

200 Finally, a protein-protein interaction analysis was performed with the top 100 nodes
201 obtained after network diffusion using the STRING database (v 11.5)(Szklarczyk et al.,
202 2019). The results were visualised with the help of Cytoscape software (v 3.9.1)(Shannon
203 et al., 2003).

204

205 # RESULTS:

206 ## *ALMS1* and *BBS1* depletion alters the
207 phosphorylation of several proteins upon TGF-β1
208 ligand stimulation:

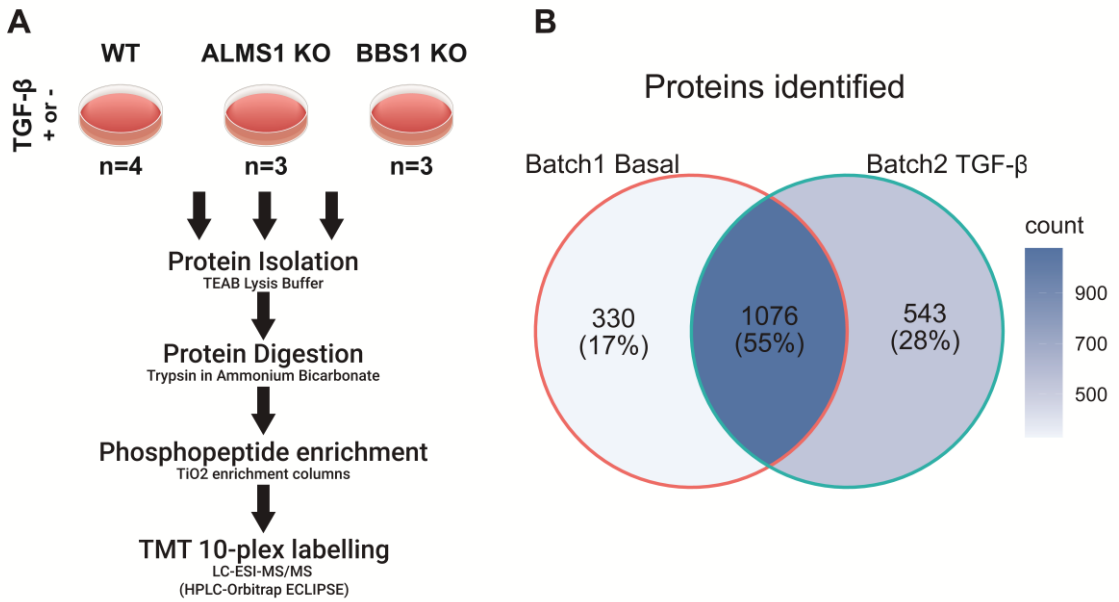


209

210 **Figure 1.** Experimental design of the phosphoproteome in basal and TGF-β-stimulated
211 BJ-5ta. **(A)** Protocol followed for the generation of the phosphoproteomic datasets **(B)**
212 Overlap between the proteins identified in Batch 1 (Basal) and Batch 2 (TGF-β).

213 The experiment was designed using two multiplexes of 10 samples each. All samples
214 (20) were cultured without FBS 24 hours before the start of the experiment. The batch
215 1 contains all samples without TGF-β1 stimulation, while batch 2 contains all samples
216 stimulated for 30 minutes with TGF-β1 **(Figure 1A-B)**. LC-MS/MS analysis identified a
217 total of 2,720 phosphopeptides (1,406 proteins) in batch 1 (without stimulation) and
218 3,317 phosphopeptides (1,619 proteins) in batch 2 (with stimulation), 1076 common
219 proteins were identified in both batches **(Figure 1B)**. Of the total peptides/proteins
220 identified, 50-60% were quantified in all samples of at least one condition (731 proteins
221 in batch 1 and 960 in batch 2) **(Figure S1 C-F)**.

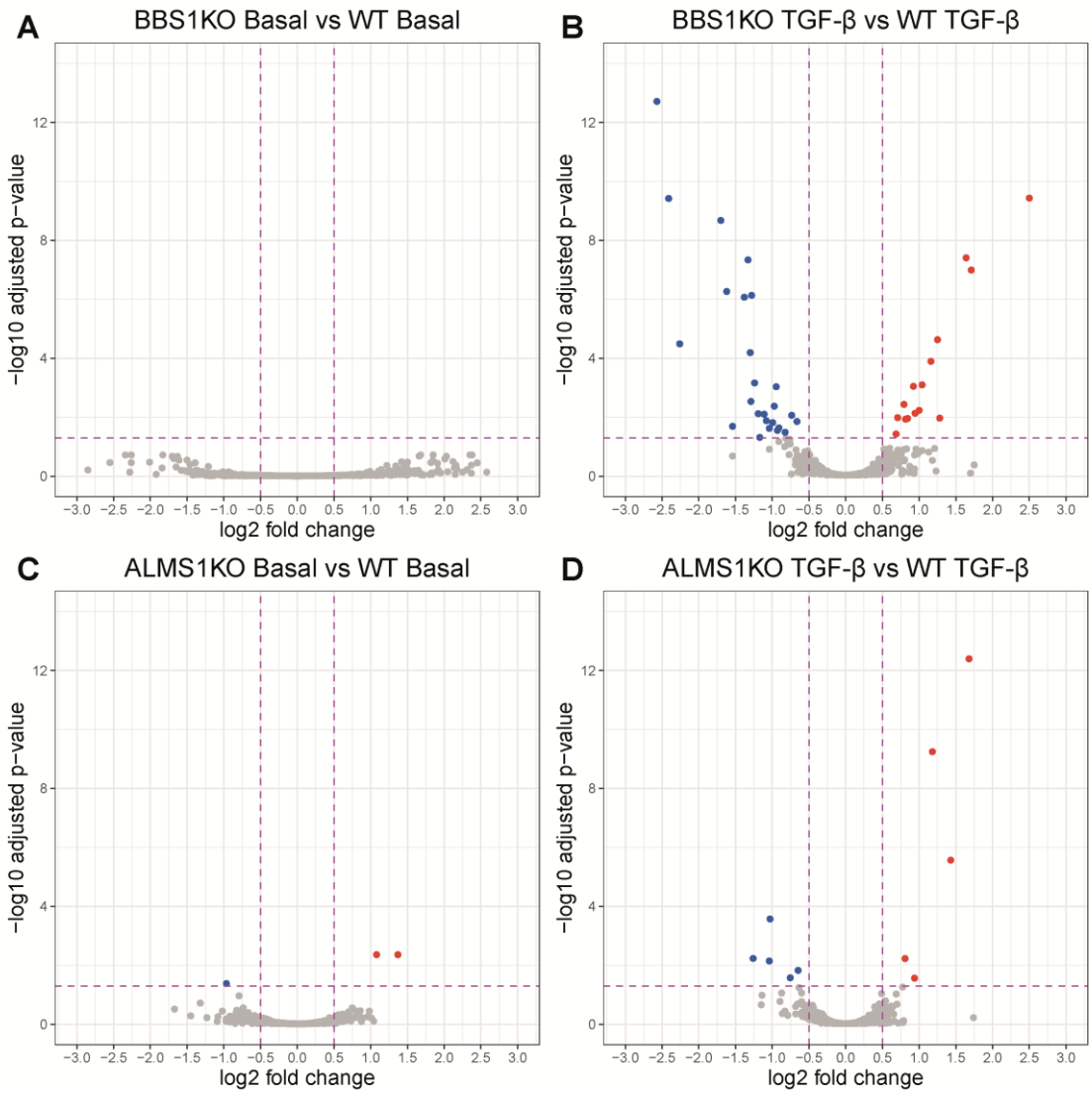


**Figure 2.** Differential phosphorylation analysis showed alterations in protein activation after TGF-β stimulation. **(A)** Volcano-plot of differentially phosphorylated proteins (FDR < 0.05) in *BBS1* knockout before TGF-β stimulation **(B)** Volcano-plot of differentially phosphorylated proteins (FDR < 0.05) in *BBS1* knockout after TGF-β stimulation **(C)** Volcano-plot of differentially phosphorylated proteins (FDR < 0.05) in *ALMS1* knockout before TGF-β stimulation **(D)** Volcano-plot of differentially phosphorylated proteins (FDR < 0.05) in *ALMS1* knockout after TGF-β stimulation.

After differential phosphorylation analysis, no significant proteins were detected in batch 1 for *BBS1* knockout (BBS1KO) and 3 significant proteins were detected in the case of *ALMS1* knockout (ALMS1KO) **(Figure 2A-C)**. Results from batch 2 showed 41 significant proteins in BBS1KO and 10 in ALMS1KO **(Figure 2B-D)**.

# Network diffusion highlights the involvement of *ALMS1* and *BBS1* in processes coordinated by the TGF-β pathway:

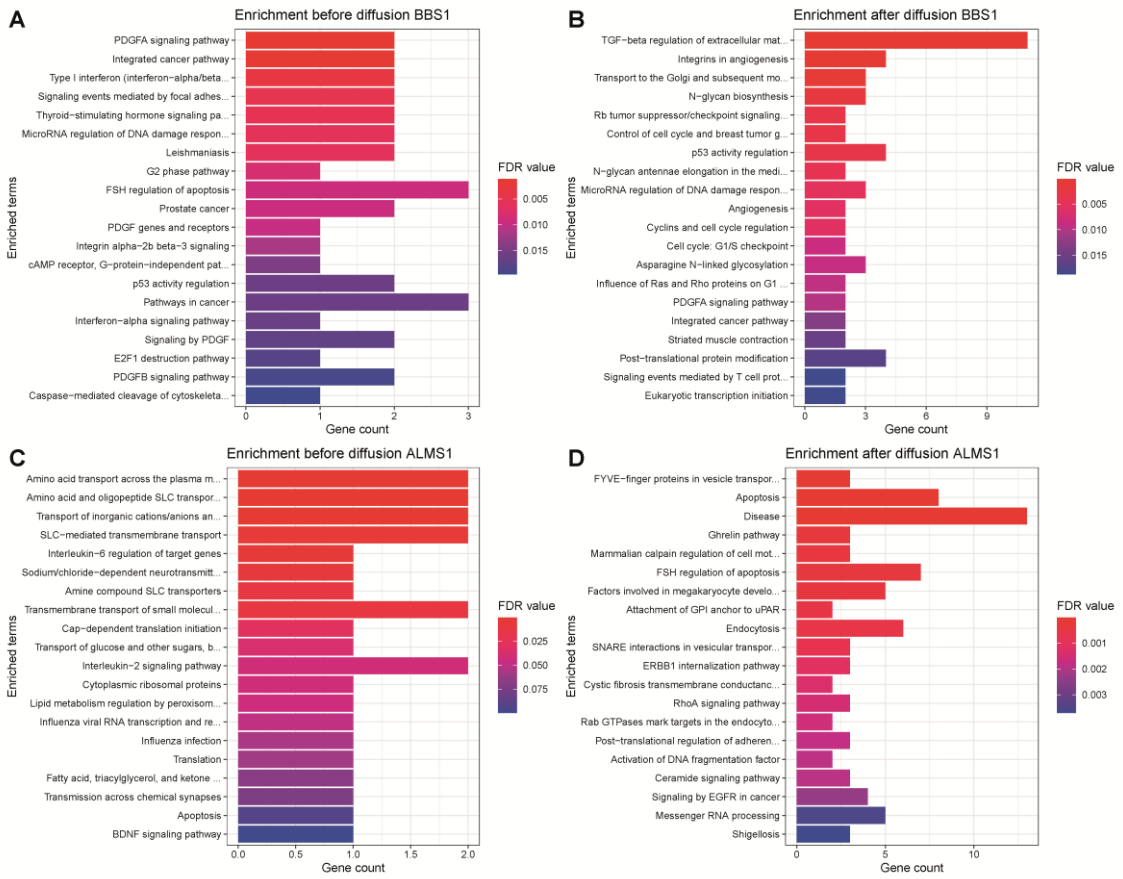


**Figure 3.** Enrichment analysis after network diffusion reveals processes controlled by TGF-β such as endocytosis, apoptosis, or extracellular matrix. **(A)** Over-representation analysis (ORA) of differentially phosphorylated proteins in the *BBS1* knockout before network diffusion. **(B)** Over-representation analysis (ORA) of top 100 most significant proteins in the *BBS1* knockout after network diffusion. **(C)** Over-representation analysis (ORA) of differentially phosphorylated proteins in the *ALMS1* knockout before network diffusion. **(D)** Over-representation analysis (ORA) of top 100 most significant proteins in the *ALMS1* knockout after network diffusion.

Differentially phosphorylated proteins after TGF-β1 stimulation were used for network diffusion analysis. Subsequently, an over-representation analysis (ORA) was performed

to determine the cellular pathways and processes related to these proteins **(Figure 3)**. Pre-diffusion ORA was performed using the differentially detected proteins after TGF-β stimulation (only seed nodes). Random results were obtained with no relation to the TGF-β pathway **(Figure 3A, C)**. On the other hand, the ORA after diffusion was performed with the top 100 nodes with the highest RWR score **(methods)**. Obtaining processes related to the TGF-β regulation of the extracellular matrix in the case of BBS1KO and endocytosis and apoptosis in the case of ALMS1KO **(Figure 3B, D)**.

# Analysis of protein-protein interactions involves CDC42 and several RAB proteins in the alterations of TGF-β signalling in *ALMS1* and CDK2 in *BBS1*:

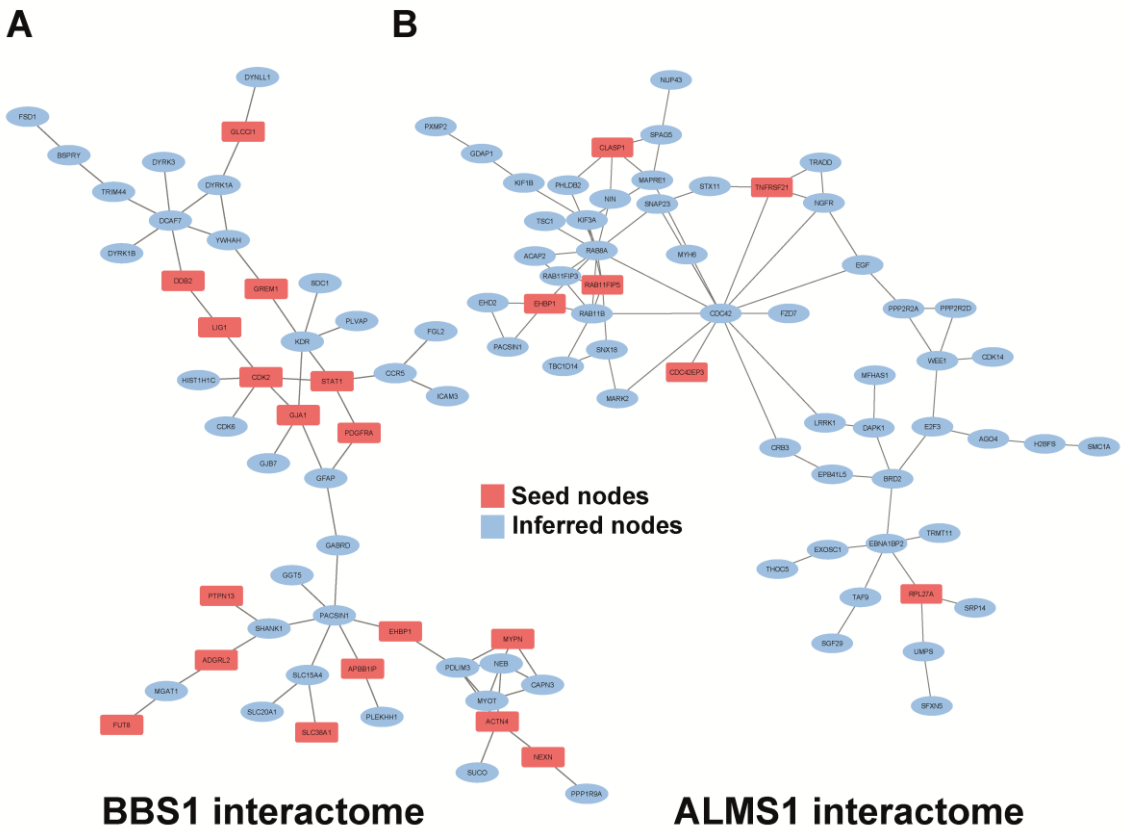


**Figure 4.** Protein-protein interaction analysis highlights CDK2 and DCAF7 as the central nodes of the *BBS1* interactome and CDC42 as the central node of the *ALMS1* interactome. Red nodes represent the differentially phosphorylated proteins that were detected in the first analysis. Blue nodes represent the nodes inferred by the random

263 walk with restart (RWR) algorithm. **(A)** Interactome of the top 100 most significant
264 proteins after network diffusion in the *BBS1* knockout. **(B)** Interactome of the top 100
265 most significant proteins after network diffusion in the *ALMS1* knockout.

266 Using the top 100 most significant proteins obtained after network diffusion, an analysis
267 of protein-protein interactions was performed. In the case of BBS1KO, CDK2 (seed
268 node), a key regulator of the cell cycle, was one of the most interconnected nodes,
269 highlighting its central role in this interactome. Another notable protein in BBS1KO was
270 *DCAF7*, one of the most interconnected of the inferred nodes **(Figure 4A)**. On the other
271 hand, in the case of ALMS1KO, CDC42, a key regulator of cell cycle and migration
272 processes, was found to be one of the most interconnected nodes in the network,
273 highlighting its central role in the deregulated interactome of this model. It also
274 highlights the highly interconnected cluster of RAB proteins such as RAB11 and RAB8
275 that play an important role in endocytosis **(Figure 4B)**.

276

# DISCUSSION:

The TGF-β pathway is one of the main signalling pathways regulated by the primary cilium (Clement et al., 2013; Pedersen et al., 2016; Christensen et al., 2017; Anvarian et al., 2019). It controls processes related to cell proliferation and migration and is associated with several pathologies such as liver or kidney fibrosis, recurrent phenotypes in ciliopathies (Zhang et al., 2017; Guan et al., 2021; McConnachie et al., 2021). Despite this, few studies have attempted to link ciliary gene dysfunction with signalling alterations in the TGF-β pathway (Mönnich et al., 2018; Álvarez-Satta et al., 2021; Bea-Mascato et al., 2022b). In this study, we have applied phosphoproteomics to determine alterations in the TGF-β signalling pathway in two model ciliopathies, ALMS and BBS. We have further elucidated the regulation of the TGF-β pathway in ALMS and established for the first time the link between the TGF-β pathway and BBS (Álvarez-Satta et al., 2021; Bea-Mascato et al., 2022b).

Phosphoproteomics is an approach that allows the global analysis of the activation of the cellular interactome. However, like any novel technique, it has several limitations, since the phosphoproteome is estimated at 30% of the total proteome and current enrichment techniques have a recovery of 1-3% of the total amount of starting sample (Low et al., 2021; Urban, 2022). The first limitation is due to a large amount of starting material needed to obtain the first data. The recommended starting material required is usually a minimum of 600µg-1mg of protein lysate (Solari et al., 2015). This is affordable when working with cell culture, but very complicated when working with tissue samples. This makes it necessary to develop techniques that increase the enrichment yield and allow the use of less starting material. Phosphoproteomics data are usually scarce and noisy, requiring the development of statistical techniques and analysis methodologies that allow robust inference from the data initially obtained (Solari et al., 2015). Furthermore, the nature of the data generated by current phosphoproteomics techniques introduces a bias in that kinases have only been identified from less than 5% of the phosphoproteome, and functional assignments of phosphosites are almost negligible (Needham et al., 2019). Currently, 90% of the phosphorylation sites have been assigned to 20% of the kinases, resulting in more than

307 150 kinases that do not have a single known substrate (Needham et al., 2019). This has
308 been named the dark phosphoproteome.

309 In this article, we designed and applied a pipeline that allowed us to obtain a global view
310 of the processes altered in the TGF-β pathway by inhibiting two ciliary genes, *ALMS1* and
311 *BBS1*. In the case of *ALMS1*, we found that the altered processes were mainly related to
312 endocytosis and apoptosis. The role of *ALMS1* in endocytotic and apoptosis processes
313 has already been established in the past (Zulato et al., 2011; Collin et al., 2012; Leitch et
314 al., 2014; Jaykumar et al., 2018; Bea-Mascato et al., 2022b). However, this is the first
315 time that these alterations in endocytosis and apoptosis could be related to the TGF-β
316 signalling pathway affecting the activation of RAB11FIP5 (seed node) and other related
317 proteins such as RAB8A and RAB11B (inferred nodes) among others. In addition, the
318 relationship of CDC42 in this interactome has also been established through CDC42EP3,
319 a CDC42 effector protein that is under-phosphorylated in the differentially
320 phosphorylated proteins detected in the differential analysis. CDC42 plays a key role in
321 cell polarity and regulation of mitosis (Witte et al., 2017; Moran et al., 2019; Rich-
322 Robinson et al., 2021). CDC42EP3 acts downstream of CDC42 and regulates the
323 rearrangement of the actin and septin cytoskeleton (Farrugia and Calvo, 2016). Cell cycle
324 disorders and cytoskeleton alterations are common phenotypes in *ALMS1*-depleted
325 cells, so a dysfunction of CDC42 and CDC42EP3 could be a possible cause of them (Zulato
326 et al., 2011; Collin et al., 2012; Shenje et al., 2014; Bea-Mascato et al., 2022b).

327 *BBS1* gene inhibition altered the phosphorylation of 41 proteins after TGF-β stimulation.
328 Following network diffusion, these proteins were found to be mainly involved in the
329 regulation of the extracellular matrix *via* the TGF-β pathway. Alterations of TGF-β
330 signalling have already been described when inhibiting other ciliary genes such as
331 *ALMS1* or *CEP128*, but never for the *BBS1* gene (Mönnich et al., 2018; Álvarez-Satta et
332 al., 2021; Bea-Mascato et al., 2022b). The main nodes of the interactome obtained from
333 the phosphoproteome were the *DCAF7*, *CDK2* and PDGFRA genes. In the case of *DCAF7*,
334 this gene acts by up-regulating *EDN1* and *GLI1* (Morita et al., 2006; Nissen et al., 2006).
335 In fibroblasts, *EDN1* is involved in the regulation of proliferative and fibrosis processes
336 related to diseases such as chronic kidney disease (CKD) (Arfian et al., 2020; Zhang et al.,
337 2020), while *GLI1* is one of the main transcription factors regulating signalling through

338 the SHh pathway (Dahmane et al., 1997; Lee et al., 1997). Moreover, SHh/GLI1 axis is
339 implicated in EMT-mediated migration regulation and *GLI1* can be regulated by the
340 SMAD-dependent TGF-β pathway in a non-canonical manner (Dennler et al., 2007; Peng
341 et al., 2019). CDK2 and PDGFRA appear under-phosphorylated, as these two proteins
342 regulate key processes such as mitosis and cell proliferation, a first indication that the
343 lack of *BBS1* prevents cells from proliferating properly by stimulating the TGF-β pathway
344 (Elling et al., 2011; Spencer et al., 2013; Li et al., 2018).

# 345 CONCLUSION:

346 In conclusion, the depletion of ciliary genes such as *ALMS1* and *BBS1* alters signal
347 transduction through the TGF-β pathway, altering processes such as endocytosis and
348 apoptosis in the case of *ALMS1* and the regulation of the extracellular matrix in the case
349 of *BBS1*. These phenomena could be explained by alterations affecting the inhibition of
350 CDCD42 in the case of *ALMS1* or CDK2 and DCAF7 in the case of *BBS1*.

351 **Author Contributions:** BB-M, DV designed the study. BB-M performed the experiments
352 and analysis. EP led the design of the analysis pipeline for differential phosphorylation
353 and network diffusion. GG and IP-S supervised and assisted in the analysis. CS performed
354 the screening and characterisation of clones for the *BBS1* KO model. All authors wrote
355 the manuscript and provided approval for publication.

356 **Funding:** This work was funded by Instituto de Salud Carlos III de Madrid FIS project
357 PI15/00049 and PI19/00332, Xunta de Galicia (Centro de Investigación de Galicia CINBIO
358 2019-2022) Ref. ED431G-2019/06, Consolidación e estructuración de unidades de
359 investigación competitivas e outras accións de fomento (ED431C-2018/54). Brais Bea-
360 Mascato (FPU17/01567) and Carlos Solarat (FPU 19/00175) were supported by graduate
361 studentship awards (FPU predoctoral fellowships) from the Spanish Ministry of
362 Education, Culture and Sports. Brais Bea-Mascato was also supported by an EMBL
363 Corporate Partnership Programme Scientific Visitors Fellowship.

364 **Informed Consent Statement:** Not Apply.

365 **Data Availability Statement:** Data are available via ProteomeXchange with the identifier
366 PXD037573.

**Code Availability Statement:** The code used in this study can be consulted on the GitHub repository https://github.com/BreisOne/phosphoproteome_pipeline.

**Acknowledgements:** We sincerely thank the Proteomics and Genomics services from Centro de Apoyo Científico-Tecnológico a la Investigación (CACTI) of University of Vigo and its specialists Paula Álvarez Chaver, Ángel Sebastián Comesaña, Verónica Outeiriño and Manuel Marcos for their guidance and advise. We also thank Mercedes Peleteiro Olmedo from Centro de Investigacións Biomédicas (CINBIO) from University of Vigo for the flow cytometry service.

**Conflicts of Interest:** The authors declare no conflict of interest. The funders had no role in the design of the study; in the collection, analyses, or interpretation of data; in the writing of the manuscript, or in the decision to publish the results.

# REFERENCES:


Aliferis, K., Hellé, S., Gyapay, G., Duchatelet, S., Stoetzel, C., Mandel, J. L., et al. (2012). Differentiating Alström from Bardet-Biedl syndrome (BBS) using systematic ciliopathy genes sequencing. *Ophthalmic Genet.* 33, 18–22. doi: 10.3109/13816810.2011.620055.

Álvarez-Satta, M., Lago-Docampo, M., Bea-Mascato, B., Solarat, C., Castro-Sánchez, S., Christensen, S. T., et al. (2021). ALMS1 Regulates TGF-β Signaling and Morphology of Primary Cilia. *Front. Cell Dev. Biol.* 9, 112. Available at: https://www.frontiersin.org/article/10.3389/fcell.2021.623829.

Anvarian, Z., Mykytyn, K., Mukhopadhyay, S., Pedersen, L. B., and Christensen, S. T. (2019). Cellular signalling by primary cilia in development, organ function and disease. *Nat. Rev. Nephrol.* 15, 199–219. doi: 10.1038/s41581-019-0116-9.

Arfian, N., Suzuki, Y., Hartopo, A. B., Anggorowati, N., Nugrahaningsih, D. A. A., and Emoto, N. (2020). Endothelin converting enzyme-1 (ECE-1) deletion in association with Endothelin-1 downregulation ameliorates kidney fibrosis in mice. *Life Sci.* 258, 118223. doi: 10.1016/J.LFS.2020.118223.

Baig, S., Paisey, R., Dawson, C., Barrett, T., Maffei, P., Hodson, J., et al. (2020). Defining renal phenotype in Alström syndrome. *Nephrol. Dial. Transplant* 35, 994–1001. doi: 10.1093/ndt/gfy293.

Bea-Mascato, B., Gómez-Castañeda, E., Sánchez-Corrales, Y. E., Castellano, S., and Valverde, D. (2022a). Loss of the centrosomal protein ALMS1 alters lipid metabolism and the regulation of extracellular matrix-related processes. *bioRxiv*, 2022.11.02.514847. doi: 10.1101/2022.11.02.514847.

Bea-Mascato, B., Neira-Goyanes, E., Iglesias-Rodríguez, A., and Valverde, D. (2022b). Depletion of ALMS1 affects TGF-β signalling pathway and downstream processes such as cell migration and adhesion capacity. *Front. Mol. Biosci.* 0, 1085. doi: 10.1101/2021.12.19.473196.

Berbari, N. F., O'Connor, A. K., Haycraft, C. J., and Yoder, B. K. (2009). The Primary Cilium

406 as a Complex Signaling Center. *Curr. Biol.* 19, R526–R535. doi:
407 10.1016/J.CUB.2009.05.025.

408 Christensen, S. T., Clement, C. A., Satir, P., and Pedersen, L. B. (2012). Primary cilia and
409 coordination of receptor tyrosine kinase (RTK) signalling. *J. Pathol.* 226, 172–184.
410 doi: 10.1002/path.3004.

411 Christensen, S. T., Morthorst, S. K., Mogensen, J. B., and Pedersen, L. B. (2017). Primary
412 Cilia and Coordination of Receptor Tyrosine Kinase (RTK) and Transforming Growth
413 Factor β (TGF-β) Signaling. *Cold Spring Harb. Perspect. Biol.* 9, a028167. doi:
414 10.1101/CSHPERSPECT.A028167.

415 Clement, C. A., Ajbro, K. D., Koefoed, K., Vestergaard, M. L., Veland, I. R., Henriques de
416 Jesus, M. P. R., et al. (2013). TGF-β signaling is associated with endocytosis at the
417 pocket region of the primary cilium. *Cell Rep.* 3, 1806–14. doi:
418 10.1016/j.celrep.2013.05.020.

419 Collin, G. B., Marshall, J. D., Ikeda, A., So, W. V., Russell-Eggitt, I., Maffei, P., et al. (2002).
420 Mutations in ALMS1 cause obesity, type 2 diabetes and neurosensory degeneration
421 in Alström syndrome. *Nat. Genet.* 31, 74–8. doi: 10.1038/ng867.

422 Collin, G. B., Marshall, J. D., King, B. L., Milan, G., Maffei, P., Jagger, D. J., et al. (2012).
423 The Alström syndrome protein, ALMS1, interacts with α-actinin and components of
424 the endosome recycling pathway. *PLoS One* 7, e37925–e37925. doi:
425 10.1371/journal.pone.0037925.

426 Csardi, G., and Nepusz, T. (2006). The igraph software package for complex network
427 research. *InterJournal, complex Syst.* 1695, 1–9.

428 Dahmane, N., Lee, J., Robins, P., Heller, P., and Ruiz I Altaba, A. (1997). Activation of the
429 transcription factor Gli1 and the Sonic hedgehog signalling pathway in skin
430 tumours. *Nat. 1997 3896653* 389, 876–881. doi: 10.1038/39918.

431 Dennler, S., André, J., Alexaki, I., Li, A., Magnaldo, T., Ten Dijke, P., et al. (2007). Induction
432 of Sonic Hedgehog Mediators by Transforming Growth Factor-β: Smad3-
433 Dependent Activation of Gli2 and Gli1 Expression In vitro and In vivo. *Cancer Res.*
434 67, 6981–6986. doi: 10.1158/0008-5472.CAN-07-0491.

435 Elling, C., Erben, P., Walz, C., Frickenhaus, M., Schemionek, M., Stehling, M., et al. (2011).
436 Novel imatinib-sensitive PDGFRA-activating point mutations in hypereosinophilic
437 syndrome induce growth factor independence and leukemia-like disease. *Blood*
438 117, 2935–2943. doi: 10.1182/BLOOD-2010-05-286757.

439 Farrugia, A. J., and Calvo, F. (2016). Cdc42 regulates Cdc42EP3 function in cancer-
440 associated fibroblasts. *http://dx.doi.org/10.1080/21541248.2016.1194952* 8, 49–
441 57. doi: 10.1080/21541248.2016.1194952.

442 Finnson, K. W., Almadani, Y., and Philip, A. (2020). Non-canonical (non-SMAD2/3) TGF-β
443 signaling in fibrosis: Mechanisms and targets. *Semin. Cell Dev. Biol.* 101, 115–122.
444 doi: 10.1016/J.SEMCDB.2019.11.013.

445 Forsythe, E., and Beales, P. L. (2012). Bardet–Biedl syndrome. *Eur. J. Hum. Genet. 2013*
446 *211* 21, 8–13. doi: 10.1038/ejhg.2012.115.

447 Forsythe, E., Kenny, J., Bacchelli, C., and Beales, P. L. (2018). Managing Bardet-Biedl
448 syndrome-now and in the future. *Front. Pediatr.* 6, 23. doi:
449 10.3389/FPED.2018.00023/XML/NLM.

450 Gasior, K., Wagner, N. J., Cores, J., Caspar, R., Wilson, A., Bhattacharya, S., et al. (2019).
451 The role of cellular contact and TGF-beta signaling in the activation of the epithelial
452 mesenchymal transition (EMT). *Cell Adhes. Migr.* 13, 63–75. doi:
453 10.1080/19336918.2018.1526597.

454 Gerdes, J. M., Davis, E. E., and Katsanis, N. (2009). The Vertebrate Primary Cilium in
455 Development, Homeostasis, and Disease. *Cell* 137, 32. doi:
456 10.1016/J.CELL.2009.03.023.

457 Guan, Y., Enejder, A., Wang, M., Fang, Z., Cui, L., Chen, S. Y., et al. (2021). A human multi-
458 lineage hepatic organoid model for liver fibrosis. *Nat. Commun. 2021 121* 12, 1–15.
459 doi: 10.1038/s41467-021-26410-9.

460 Hamidi, A., Song, J., Thakur, N., Itoh, S., Marcusson, A., Bergh, A., et al. (2017). TGF-β
461 promotes PI3K-AKT signaling and prostate cancer cell migration through the TRAF6-
462 mediated ubiquitylation of p85α. *Sci. Signal.* 10. doi: 10.1126/SCISIGNAL.AAL4186.

463 Harispe, S., Ranwez, S., Janaqi, S., and Montmain, J. (2014). The semantic measures
464 library and toolkit: fast computation of semantic similarity and relatedness using
465 biomedical ontologies. *Bioinformatics* 30, 740–742. doi:
466 10.1093/BIOINFORMATICS/BTT581.

467 Hearn, T. (2018). ALMS1 and Alström syndrome: a recessive form of metabolic,
468 neurosensory and cardiac deficits. *J. Mol. Med.* doi: 10.1007/s00109-018-1714-x.

469 Hearn, T., Spalluto, C., Phillips, V. J., Renforth, G. L., Copin, N., Hanley, N. A., et al. (2005).
470 Subcellular Localization of ALMS1 Supports Involvement of Centrosome and Basal
471 Body Dysfunction in the Pathogenesis of Obesity, Insulin Resistance, and Type 2
472 Diabetes. *Diabetes* 54, 1581 LP – 1587. doi: 10.2337/diabetes.54.5.1581.

473 Ishikawa, H., and Marshall, W. F. (2011). Ciliogenesis: building the cell's antenna. *Nat.*
474 *Rev. Mol. Cell Biol.* 12, 222–234. doi: 10.1038/NRM3085.

475 Jain, S., and Bader, G. D. (2010). An improved method for scoring protein-protein
476 interactions using semantic similarity within the gene ontology. *BMC*
477 *Bioinformatics* 11, 562. doi: 10.1186/1471-2105-11-562.

478 Jaykumar, A. B., Caceres, P. S., King-Medina, K. N., Liao, T.-D., Datta, I., Maskey, D., et al.
479 (2018). Role of Alström syndrome 1 in the regulation of blood pressure and renal
480 function. *JCI insight* 3, e95076. doi: 10.1172/jci.insight.95076.

481 Klink, B. U., Gatsogiannis, C., Hofnagel, O., Wittinghofer, A., and Raunser, S. (2020).
482 Structure of the human BBSome core complex. *Elife* 9. doi: 10.7554/ELIFE.53910.

483 Köhler, S., Bauer, S., Horn, D., and Robinson, P. N. (2008). Walking the Interactome for
484 Prioritization of Candidate Disease Genes. *Am. J. Hum. Genet.* 82, 949–958. doi:
485 10.1016/J.AJHG.2008.02.013.

486 Kuleshov, M. V., Jones, M. R., Rouillard, A. D., Fernandez, N. F., Duan, Q., Wang, Z., et al.
487 (2016). Enrichr: a comprehensive gene set enrichment analysis web server 2016
488 update. *Nucleic Acids Res.* 44, W90. doi: 10.1093/NAR/GKW377.

489 Lan, H. Y. (2011). Diverse roles of TGF-β/Smads in renal fibrosis and inflammation. *Int. J.*
490 *Biol. Sci.* 7, 1056–1067. doi: 10.7150/IJBS.7.1056.

491 Lee, J., Platt, K. A., Censullo, P., and Ruiz I Altaba, A. (1997). Gli1 is a target of Sonic
492 hedgehog that induces ventral neural tube development. *Development* 124, 2537–
493 2552. doi: 10.1242/DEV.124.13.2537.

494 Leitch, C. C., Lodh, S., Prieto-Echagüe, V., Badano, J. L., and Zaghloul, N. A. (2014). Basal
495 body proteins regulate Notch signaling through endosomal trafficking. *J. Cell Sci.*
496 127, 2407–19. doi: 10.1242/jcs.130344.

497 Li, G., Vega, R., Nelms, K., Gekakis, N., Goodnow, C., McNamara, P., et al. (2007). A role
498 for Alström syndrome protein, alms1, in kidney ciliogenesis and cellular quiescence.
499 *PLoS Genet.* 3, e8. doi: 10.1371/journal.pgen.0030008.

500 Li, R., Bernau, K., Sandbo, N., Gu, J., Preissl, S., and Sun, X. (2018). Pdgfra marks a cellular
501 lineage with distinct contributions to myofibroblasts in lung maturation and injury
502 response. *Elife* 7. doi: 10.7554/ELIFE.36865.

503 Licata, L., Lo Surdo, P., Iannuccelli, M., Palma, A., Micarelli, E., Perfetto, L., et al. (2020).
504 SIGNOR 2.0, the SIGnaling Network Open Resource 2.0: 2019 update. *Nucleic Acids*
505 *Res.* 48, D504–D510. doi: 10.1093/NAR/GKZ949.

506 Low, T. Y., Mohtar, M. A., Lee, P. Y., Omar, N., Zhou, H., and Ye, M. (2021). Widening the
507 bottleneck of phosphoproteomics: evolving strategies for phosphopeptide
508 enrichment. *Mass Spectrom. Rev.* 40, 309–333. doi: 10.1002/mas.21636.

509 Luo, K. (2017). Signaling Cross Talk between TGF-β/Smad and Other Signaling Pathways.
510 *Cold Spring Harb. Perspect. Biol.* 9, a022137. doi: 10.1101/cshperspect.a022137.

511 Marshall, J. D., Maffei, P., Collin, G. B., and Naggert, J. K. (2011). Alström syndrome:
512 genetics and clinical overview. *Curr. Genomics* 12, 225–235. doi:
513 10.2174/138920211795677912.

514 Massagué, J. (2012). TGFβ signalling in context. *Nat. Rev. Mol. Cell Biol.* 13, 616–630.
515 doi: 10.1038/nrm3434.

516 May-Simera, H. L., Wan, Q., Jha, B. S., Hartford, J., Khristov, V., Dejene, R., et al. (2018).
517 Primary Cilium-Mediated Retinal Pigment Epithelium Maturation Is Disrupted in
518 Ciliopathy Patient Cells. *Cell Rep.* 22, 189–205. doi: 10.1016/j.celrep.2017.12.038.

519 McConnachie, D. J., Stow, J. L., and Mallett, A. J. (2021). Ciliopathies and the Kidney: A
520 Review. *Am. J. Kidney Dis.* 77, 410–419. doi: 10.1053/J.AJKD.2020.08.012.

521 Meng, X. M., Nikolic-Paterson, D. J., and Lan, H. Y. (2014). Inflammatory processes in
522 renal fibrosis. *Nat. Rev. Nephrol. 2014 109* 10, 493–503. doi:
523 10.1038/nrneph.2014.114.

524 Meyer, J. R., Krentz, A. D., Berg, R. L., Richardson, J. G., Pomeroy, J., Hebbring, S. J., et al.
525 (2022). Kidney failure in Bardet–Biedl syndrome. *Clin. Genet.* 101, 429–441. doi:
526 10.1111/CGE.14119.

527 Mönnich, M., Borgeskov, L., Breslin, L., Jakobsen, L., Rogowski, M., Doganli, C., et al.
528 (2018). CEP128 Localizes to the Subdistal Appendages of the Mother Centriole and
529 Regulates TGF-β/BMP Signaling at the Primary Cilium. *Cell Rep.* 22, 2584–2592. doi:
530 10.1016/J.CELREP.2018.02.043.

531 Moran, K. D., Kang, H., Araujo, A. V., Zyla, T. R., Saito, K., Tsygankov, D., et al. (2019).
532 Cell-cycle control of cell polarity in yeast. *J. Cell Biol.* 218, 171–189. doi:
533 10.1083/JCB.201806196.

534 Morita, K., Celso, C. Lo, Spencer-Dene, B., Zouboulis, C. C., and Watt, F. M. (2006). HAN11
535 binds mDia1 and controls GLI1 transcriptional activity. *J. Dermatol. Sci.* 44, 11–20.
536 doi: 10.1016/J.JDERMSCI.2006.06.001.

537 Needham, E. J., Parker, B. L., Burykin, T., James, D. E., and Humphrey, S. J. (2019).
538 Illuminating the dark phosphoproteome. *Sci. Signal.* 12. doi:
539 10.1126/SCISIGNAL.AAU8645/SUPPL_FILE/AAU8645_SM.PDF.

540 Nissen, R. M., Amsterdam, A., and Hopkins, N. (2006). A zebrafish screen for craniofacial
541 mutants identifies wdr68 as a highly conserved gene required for endothelin-1
542 expression. *BMC Dev. Biol.* 6, 1–17. doi: 10.1186/1471-213X-6-28/TABLES/3.

543 Orchard, S., Ammari, M., Aranda, B., Breuza, L., Briganti, L., Broackes-Carter, F., et al.
544 (2014). The MIntAct project—IntAct as a common curation platform for 11
545 molecular interaction databases. *Nucleic Acids Res.* 42, D358–D363. doi:
546 10.1093/NAR/GKT1115.

547 Pedersen, L. B., Mogensen, J. B., and Christensen, S. T. (2016). Endocytic Control of
548 Cellular Signaling at the Primary Cilium. *Trends Biochem. Sci.* 41, 784–797. doi:
549 10.1016/J.TIBS.2016.06.002.

550 Peng, L., Yang, C., Yin, J., Ge, M., Wang, S., Zhang, G., et al. (2019). TGF-β2 Induces Gli1
551 in a Smad3-Dependent Manner against Cerebral Ischemia/Reperfusion Injury after
552 Isoflurane Post-conditioning in Rats. *Front. Neurosci.* 13, 636. doi:
553 10.3389/FNINS.2019.00636/BIBTEX.

554 Putoux, A., Attie-Bitach, T., Martinovic, J., and Gubler, M. C. (2012). Phenotypic
555 variability of Bardet-Biedl syndrome: Focusing on the kidney. *Pediatr. Nephrol.* 27,
556 7–15. doi: 10.1007/S00467-010-1751-3/TABLES/2.

557 Reiter, J. F., and Leroux, M. R. (2017). Genes and molecular pathways underpinning
558 ciliopathies. *Nat. Rev. Mol. Cell Biol.* 18, 533–547. doi: 10.1038/nrm.2017.60.

559 Rich-Robinson, J., Russell, A., Mancini, E., and Das, M. (2021). Cdc42 reactivation at
560 growth sites is regulated by local cell-cycle-dependent loss of its GTPase-activating
561 protein Rga4 in fission yeast. *J. Cell Sci.* 134. doi: 10.1242/JCS.259291.

562 Shannon, P., Markiel, A., Ozier, O., Baliga, N. S., Wang, J. T., Ramage, D., et al. (2003).
563 Cytoscape: A Software Environment for Integrated Models of Biomolecular
564 Interaction Networks. *Genome Res.* 13, 2498–2504. doi: 10.1101/GR.1239303.

565 Shenje, L. T., Andersen, P., Halushka, M. K., Lui, C., Fernandez, L., Collin, G. B., et al.
566 (2014). Mutations in Alström protein impair terminal differentiation of
567 cardiomyocytes. *Nat. Commun.* 5, 3416. doi: 10.1038/ncomms4416.

568 Singh, S., Gui, M., Koh, F., Yip, M. C. J., and Brown, A. (2020). Structure and activation
569 mechanism of the BBSome membrane protein trafficking complex. *Elife* 9. doi:
570 10.7554/ELIFE.53322.

571 Solari, F. A., Dell'Aica, M., Sickmann, A., and Zahedi, R. P. (2015). Why
572 phosphoproteomics is still a challenge. *Mol. Biosyst.* 11, 1487–1493. doi:
573 10.1039/C5MB00024F.

574 Spencer, S. L., Cappell, S. D., Tsai, F. C., Overton, K. W., Wang, C. L., and Meyer, T. (2013).

575 The Proliferation-Quiescence Decision Is Controlled by a Bifurcation in CDK2
576 Activity at Mitotic Exit. *Cell* 155, 369–383. doi: 10.1016/J.CELL.2013.08.062.

577 Szklarczyk, D., Gable, A. L., Lyon, D., Junge, A., Wyder, S., Huerta-Cepas, J., et al. (2019).
578 STRING v11: protein–protein association networks with increased coverage,
579 supporting functional discovery in genome-wide experimental datasets. *Nucleic*
580 *Acids Res.* 47, D607–D613. doi: 10.1093/NAR/GKY1131.

581 Tong, H., Faloutsos, C., and Pan, J. (2006). Fast Random Walk with Restart and Its
582 Applications. in *Sixth International Conference on Data Mining (ICDM'06)*, 613–622.
583 doi: 10.1109/ICDM.2006.70.

584 Türei, D., Korcsmáros, T., and Saez-Rodriguez, J. (2016). OmniPath: guidelines and
585 gateway for literature-curated signaling pathway resources. *Nat. Methods 2016*
586 *1312* 13, 966–967. doi: 10.1038/nmeth.4077.

587 Urban, J. (2022). A review on recent trends in the phosphoproteomics workflow. From
588 sample preparation to data analysis. *Anal. Chim. Acta* 1199, 338857. doi:
589 10.1016/J.ACA.2021.338857.

590 Waldman, M., Han, J. C., Reyes-Capo, D. P., Bryant, J., Carson, K. A., Turkbey, B., et al.
591 (2018). Alström syndrome: Renal findings in correlation with obesity, insulin
592 resistance, dyslipidemia and cardiomyopathy in 38 patients prospectively
593 evaluated at the NIH clinical center. *Mol. Genet. Metab.* 125, 181–191. doi:
594 10.1016/j.ymgme.2018.07.010.

595 Waters, A. M., and Beales, P. L. (2011). Ciliopathies: An expanding disease spectrum.
596 *Pediatr. Nephrol.* 26, 1039–1056. doi: 10.1007/S00467-010-1731-7/FIGURES/5.

597 Witte, K., Strickland, D., and Glotzer, M. (2017). Cell cycle entry triggers a switch
598 between two modes of Cdc42 activation during yeast polarization. *Elife* 6. doi:
599 10.7554/ELIFE.26722.

600 Zhang, L., Chen, L., Gao, C., Chen, E., Lightle, A. R., Foulke, L., et al. (2020). Loss of Histone
601 H3 K79 Methyltransferase Dot1l Facilitates Kidney Fibrosis by Upregulating
602 Endothelin 1 through Histone Deacetylase 2. *J. Am. Soc. Nephrol.* 31, 337–349. doi:
603 10.1681/ASN.2019070739.

604 Zhang, X., Smits, A. H., van Tilburg, G. B., Ovaa, H., Huber, W., and Vermeulen, M. (2018).
605 Proteome-wide identification of ubiquitin interactions using UbIA-MS. *Nat. Protoc.*
606 13, 530–550. doi: 10.1038/nprot.2017.147.

607 Zhang, Y., Alexander, P. B., and Wang, X. F. (2017). TGF-β family signaling in the control
608 of cell proliferation and survival. *Cold Spring Harb. Perspect. Biol.* 9. doi:
609 10.1101/cshperspect.a022145.

610 Zulato, E., Favaretto, F., Veronese, C., Campanaro, S., Marshall, J. D., Romano, S., et al.
611 (2011). ALMS1-deficient fibroblasts over-express extra-cellular matrix components,
612 display cell cycle delay and are resistant to apoptosis. *PLoS One* 6, e19081–e19081.
613 doi: 10.1371/journal.pone.0019081.